# The mechanics of slithering locomotion

**David L. Hu[a,b,1], Jasmine Nirody[a], Terri Scott[a], and Michael J. Shelley[a]**

[a]Applied Mathematics Laboratory, Courant Institute of Mathematical Sciences, New York University, New York, NY 10003; and [b]Departments of Mechanical Engineering and Biology, Georgia Institute of Technology, Atlanta, GA 30332

In this experimental and theoretical study, we investigate the slithering of snakes on flat surfaces. Previous studies of slithering have rested on the assumption that snakes slither by pushing laterally against rocks and branches. In this study, we develop a theoretical model for slithering locomotion by observing snake motion kinematics and experimentally measuring the friction coefficients of snakeskin. Our predictions of body speed show good agreement with observations, demonstrating that snake propulsion on flat ground, and possibly in general, relies critically on the frictional anisotropy of their scales. We have also highlighted the importance of weight distribution in lateral undulation, previously difficult to visualize and hence assumed uniform. The ability to redistribute weight, clearly of importance when appendages are airborne in limbed locomotion, has a much broader generality, as shown by its role in improving limbless locomotion.

friction | locomotion | snake

Limbless creatures are slender and flexible, enabling them to use methods of locomotion that are fundamentally different from the more commonly studied flying, swimming, walking, and running used by similarly sized limbed or finned organisms. These methods can be as efficient as legged locomotion (1) and moreover are particularly versatile when moving over uneven terrain or through narrow crevices, for which the possession of limbs would be an impediment (2, 3). Limbless invertebrates such as slugs propel themselves by generating lubrication forces with their mucus-covered bodies; earthworms move by ratcheting: propulsion is achieved by engaging their hairs in the ground as they elongate and shorten their bodies (4, 5). Terrestrial snakes propel themselves by using a variety of techniques, including slithering by lateral undulation of the body, rectilinear progression by unilateral contraction/extension of their belly, concertina-like motion by folding the body as the pleats of an accordion, and sidewinding motion by throwing the body into a series of helices. This report will focus on lateral undulation, whose utility to locomotion by snakes has been previously described on the basis of push points: Snakes slither by driving their flanks laterally against neighboring rocks and branches found along the ground (6–11). This key assumption has informed numerous theoretical analyses (12–17) and facilitated the design of snake robots for search-and-rescue operations. Previous investigators (7, 9, 18, 19) have suggested that the frictional anisotropy of the snake's belly scales might play a role in locomotion over flat surfaces. The details of this friction-based process, however, remain to be understood; consequently, snake robots have been generally built to slither over flat surfaces by using passive wheels fixed to the body that resist lateral motion (18, 20–22). In this report, we present a theory for how snakes slither, or how wheelless snake robots can be designed to slither, on relatively featureless terrain, such as sand or bare rock, which do not provide obvious push points.

## Model

We model snakes (Fig. 1 *A* and *B*) as inextensible 1-dimensional curves $X(s,t) = (x(s,t),y(s,t))$ of fixed length $L$ and uniform mass per unit length $\nu$ (Fig. 1C). Here, $s$ is the curve arc length measured from the head, and $t$ is time. The snakes' motion arises through balancing body inertia at each point along the curve with

the sum of frictional forces per unit length, $f_{fric}$, and internal forces, $f_{int}$, generated by the snakes. That is,

$$\nu \ddot{X} = f_{fric} + f_{int}, \qquad [1]$$

where $\ddot{X}$ is the acceleration at each point along the snake's body. To avoid complex issues of muscle and tissue modeling, $f_{int}$ is determined to be that necessary for the model snake to produce the observed shape kinematics. We use a sliding friction law in which the friction force per unit length is $f = -\mu^k \nu g \hat{u}$, where $\mu^k$ is the sliding friction coefficient, $\hat{u} = u/|u|$ is the velocity direction, and $\nu g$ is the normal force per unit length applied by the snake to the ground. We assume that the sliding friction coefficients $\mu_k$ are equal (or at least proportional) to the corresponding static ones we have measured [$(\mu_f^k, \mu_t^k, \mu_b^k) = \alpha(\mu_f, \mu_t, \mu_b)$]. Applied to incorporate our measured frictional anisotropies, we model $f_{fric}$ simply as a weighted average of independent frictional responses to motions in the forwards ($\hat{s}$), backwards ($-\hat{s}$), and transverse directions ($\hat{n}$). That is,

$$f_{fric} = -\nu g(\mu_t^k(\hat{u} \cdot \hat{n})\hat{n} + [\mu_f^k H(\hat{u} \cdot \hat{s}) + \mu_b^k(1 - H(\hat{u} \cdot \hat{s}))]$$
$$\cdot (\hat{u} \cdot \hat{s})\hat{s}), \qquad [2]$$

where $H = \frac{1}{2}[1 + \text{sgn}(x)]$ is the Heaviside step function used to distinguish the components in the $\hat{s}$ and $-\hat{s}$ directions. Eqs. 1 and 2 can be made dimensionless by scaling lengths on the snake body length $L$ and time on the snake's period of undulation $\tau$, together with the force redefinition $f = \mu \nu g \tilde{f}$, where $\mu$ is a characteristic sliding friction coefficient, taken to be 0.2. Eq. 1 then becomes

$$Fr\ddot{X} = \tilde{f}_{fric} + \tilde{f}_{int}, \qquad [3]$$

where Fr is defined below. We prescribe the body shape in terms of body curvature $\kappa(s, t)$, which is a quantity without reference to absolute position or orientation in the plane. The force balance, Eq. 3, is used to find the dynamics of the snake center of mass $\bar{X}$ and mean orientation $\bar{\theta}$ through the requirement the total internal force and torque generated by the snake to execute its specified shape dynamics are zero. Those constraints, $\int_0^1 \tilde{f}_{int}(s)ds = \mathbf{0}$ and $\int_0^1 (X(s, t) - \bar{X}) \times f_{int}(s)ds = \mathbf{0}$, generate equations for $\ddot{\bar{X}}$ and $\ddot{\bar{\theta}}$. The resultant system of ordinary differential equations are easily evolved numerically, with the only parameters being the Froude number $Fr$, often used in modeling terrestrial locomotion (23), and the friction coefficients $\mu_{f,b,t}$. A natural definition for a mechanical efficiency is the ratio of the power to drag a straight snake to the active power mediated by friction on a slithering snake, $\eta = \bar{U}_{avg}/[\int_0^1 \tilde{f}_{fric} \cdot \dot{X} ds]_{avg}$, where the subscript avg denotes a time average over a period.

A critical parameter that arises in our theory is the so-called "Froude number," $Fr = (L/\tau^2)/\mu g$, which measures the relative importance of inertial to frictional forces (which both scale with

**APPLIED PHYSICAL SCIENCES**
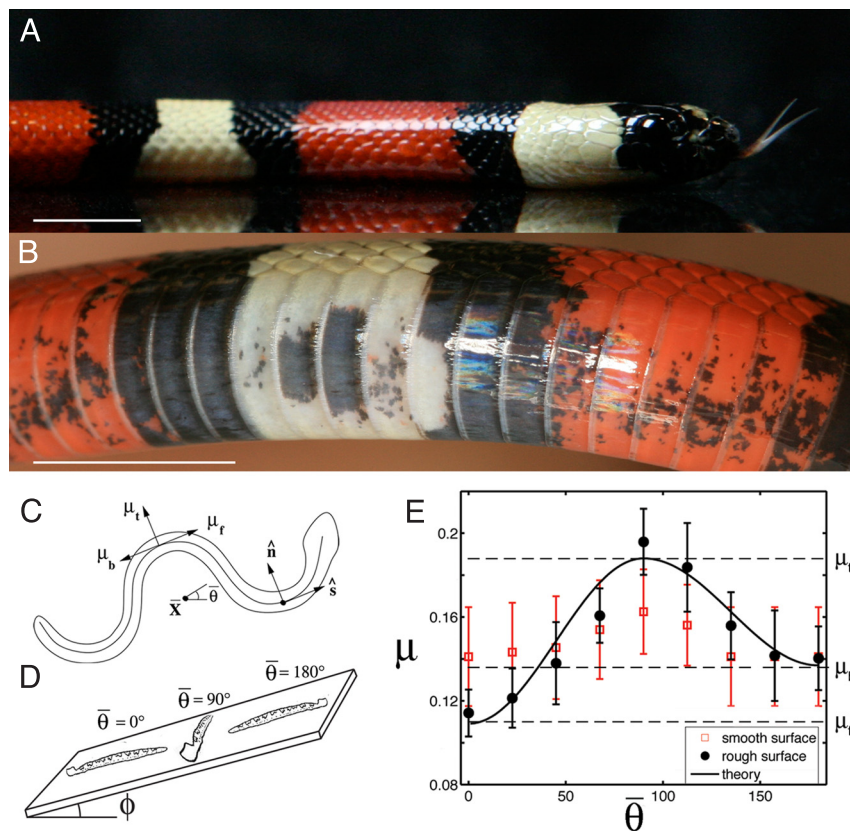
**APPLIED BIOLOGICAL SCIENCES**

**Fig. 1.** Frictional anisotropy of snakeskin. (*A* and *B*) One of the milk snakes used in our experiments (*A*) and its ventral scutes (*B*), whose orientation allows them to interlock with ground asperities. (Scale bars, 1 cm.) (*C*) Schematic diagram for our theoretical model, where $\bar{X}$ denotes the snake's center of mass, $\bar{\theta}$ its mean orientation, and $\hat{s}$ and $\hat{n}$ the tangent and normal vectors to the body, taken toward the head. (*D*) The experimental apparatus, an inclined plane, used to measure the static friction coefficient $\mu$ of unconscious snakes. (*E*) The relation between the static friction coefficient $\mu$ and angle $\bar{\theta}$ with respect to the direction of motion, for straight unconscious snakes. Filled symbols indicate measurements on cloth; open symbols, on smooth fiberboard; solid curve derived from theory (Eq. 2) by using $\mu_f = 0.11$, $\mu_t = 0.19$, and $\mu_b = 0.14$. Error bars indicate the standard deviation of measurement.

mass). From our observations, we estimate that frictional forces are an order of magnitude greater than inertial forces (i.e., $Fr \approx 0.1$, using $\mu = 0.2$; see Fig. 1), which gives the important result that, unlike most other terrestrial organisms of this size, body inertia is not central to slithering locomotion. Motion instead arises by the interaction of surface friction and internal body forces. Even the red racer (24), one of the world's fastest snakes, has $Fr \approx 1 - 1.5 (L = 60 - 130$ cm, $U = 130$ cm/s), indicating that its body inertia is not predominant. In the zero $Fr$ limit, forces are transduced directly to velocities rather than accelerations, which is also a feature of the low Reynolds number locomotion of microorganisms through a fluid (25). Another simplifying aspect for our particular model is that for low $Fr$ motion on horizontal surfaces, the dynamics depends on only 2 ratios of friction coefficients, say $\mu_f/\mu_t$ and $\mu_b/\mu_t$.

## Results

The wide overlapping belly scales of these snakes have an important function: They snag on ground asperities, a phenomenon that was audible during experiments (Fig. 1*B*). As a result, these scales provide the snake a preferred direction of sliding on surfaces of sufficient roughness and compliance, as can be shown by the clear anisotropy in friction coefficients on the cloth surface (Fig. 1*E*). The static friction coefficient $\mu$ is least if the snakes are sliding forward ($\mu_f = 0.11 \pm 0.011$), intermediate if sliding tailward ($\mu_b = 0.14 \pm 0.015$), and highest toward its flanks ($\mu_t = 0.20 \pm 0.015$). On the other hand, the smooth surface, which provides few if any asperities for the scales to catch on, shows friction coefficients that are nearly independent of orientation ($\mu_f \approx 0.14$, $\mu_t \approx 0.16$, $\mu_b \approx$

0.14). The values of these coefficients are slightly less than those measured elsewhere (7) for dead snakes on various surfaces ($\mu_f$ and $\mu_b$ between 0.24 and 1.30). We also observe that while the snakes were recovering from unconsciousness, they began twitching their scales individually. This level of control is consistent with their neuromuscular anatomy (2), which shows that each scale has its own muscular attachment.

The snake's frictional anisotropy with the surface is critical to its motion, at least on horizontal surfaces (angle of inclination $\phi = 0$). Fig. 2*a'* shows time-lapse photographs of a snake unsuccessfully attempting to slither forward when placed on a smooth surface. No such difficulties are presented when the snake is placed on the rough surface, as illustrated by Fig. 2*a"*. The snakes' motion kinematics were also filmed and digitized ($n = 20$), and the open circles in Fig. 2 *A–C* shows the measured positions of the snakes' center of mass during steady undulation, where quantities have been normalized by body length $L = 30$ cm and time normalized by period of undulation $\tau = 2$ s. It is noteworthy that whereas the body kinematics are undulatory (with a dimensionless wavelength of $0.4 \pm 0.1$ and an amplitude of $A = 0.1 \pm 0.03$), the motion of the center of mass $(\bar{X}, \bar{Y})$ is almost purely translational. The snakes' forward speeds are nearly steady ($\bar{U} = 0.22 \pm 0.08$), whereas their speeds transverse to the direction of motion are negligible ($\bar{V} = 0.0 \pm 0.03$; see Fig. 2 *A* and *B*). The snakes' mean angle of orientation $\bar{\theta}$ rotates substantially ($20 \pm 5°$) during slithering (Fig. 2*C*). We note that the snakes' undulation is not always steady, as shown by the small changes in their periods of undulation shown in Fig. 2*C*. We also observe that, at least on horizontal surfaces, the snakes are
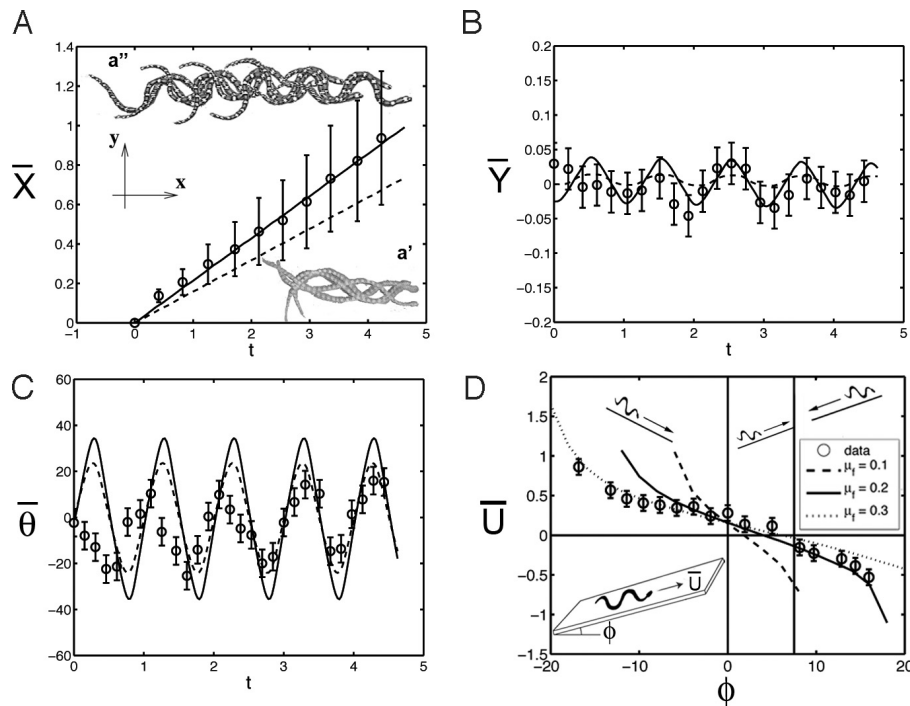
**Fig. 2.** Dynamics of snake locomotion. (*A–C*) Position ($\bar{X}$, $\bar{Y}$) and orientation $\bar{\theta}$ of the snakes on a horizontal surface. Open circles show experimental results; solid lines show the theoretical results from a lifted-snake model, dashed lines for a uniform-weight model. Error bars show the standard deviation of the measurement. (*Insets*) (*a'* and *a"*) show photographic sequences of snakes moving on smooth and rough surfaces respectively. (*D*) Snakes' forward speeds $\bar{U}$ on an plane inclined at angle $\phi$. Smooth curves represent theoretical predictions of steady-state speeds using $\mu_f$ given in the figure and frictional anisotropies of $\mu_t = 1.8\,\mu_f$, $\mu_b = 1.3\,\mu_f$. Three regimes of motion exist: for $\phi < 0°$, the snake successfully slithers downhill; for $0° < \phi < 7°$, the snake successfully slithers uphill; for $\phi > 7°$, the snake slides backwards when slithering uphill.

capable of short bursts of speed of 0.4, or nearly double its steady speed (as shown by error bars in Fig. 2*A* and in speed data for $\phi = 0$ in Fig. 2*D*).

Experiments ($n = 70$) were performed to determine the snakes' speed on cloth surfaces set at inclinations $\phi$ to the horizontal between $-20°$ and $20°$, angles corresponding to the snake slithering downhill and uphill, respectively (Fig. 2*D*). At inclinations below a critical inclination of $\phi^* = 7 \pm 2°$, the snakes successfully slither forward by lateral undulation; at inclinations of $\phi^*$, the snakes slither in place; at inclinations below $\phi^*$, the snakes attempt to slither forward but, instead, slide backward.

We now compare our experimental observations with the predictions of our theoretical model, first using our model to describe the measured frictional anisotropy. The average friction coefficients for our straight snakes are given by Eq. **2** as $\bar{\mu} = \mu_t \sin^2\bar{\theta} + [\mu_f H(\cos\bar{\theta}) + \mu_b(1 - H(\cos\bar{\theta}))]\cos^2\bar{\theta}$. By using the data in Fig. 1*D*, the least-squares estimates for the friction coefficients are $\mu_f = 0.11$, $\mu_t = 0.19$, and $\mu_b = 0.14$. Because these values provide a frictional dependence on orientation that is in approximate accordance with our data, they will be used henceforth in our simulations.

Next, we use the observed snake shape dynamics to study the motions predicted by our model. As an Ansatz, we assume snakes' undulation is described by a simple traveling wave in curvature: $\kappa(s, t) = \alpha \cos k\pi(s + t)$ (in dimensionless units). Typical values from our observation are $\alpha = 7$ and $k = 2$, which we use in our numerical simulation. First, to understand our observations of snake motion on a smooth surface, we set $\mu_f = \mu_b = \mu_t$, and find little if any locomotion of the snake. On the other hand, using the measured frictional anisotropy, we predict trajectories of the model snake on a horizontal surface fairly consistent with those observed: specifically, $\bar{Y}$ and $\bar{\theta}$ in Fig. 2 *A–C* are well accounted for, and forward

speeds $\bar{U}$ of 0.17 are lower than the mean but within the standard error found in experiments.

Our prediction of the snakes' body speeds on the incline also show good agreement with observations. Fig. 2*D* shows the measured snake speeds compared with 3 theoretical predictions given by our model, found by varying the forward friction coefficient $\mu_f$ from 0.1 to 0.3 and keeping the remaining coefficients in the ratio $\mu_t = 1.8\mu_f$, $\mu_b = 1.3\mu_f$. We find that this range of friction coefficients accounts for the trends observed.

### Discussion

Our simple theoretical model based on snake friction coefficients captures the general trends found in our experiments, although predicted speeds tend be somewhat lower than those measured. We offer several possible sources of discrepancy between observed and predicted speeds. We believe that the largest contributor to these disparities is given by the dynamic load-balancing we have observed in snake locomotion. Previous investigators (8, 9, 18) have observed that at high speeds, snakes lift the curved parts of their bodies off of the ground as they travel in lateral undulation and in sidewinding (26). This can be seen clearly in Fig. 3*A*, which shows a corn snake slithering on a mirrored surface. Through the lens of our model, we interpret this behavior as the snake dynamically distributing its weight so that its belly is periodically loaded (pressed) and unloaded (lifted), concentrating its weight on specific points of contact. We have observed that these points of contact correspond approximately to points of zero body curvature. By incorporating into the frictional force of our model a nonuniform weight distribution that concentrates weight on points of zero body curvature, we provide a mechanical rationale for body-lifting. The speeds of a lifted snake model and a uniform-weight snake model are shown by the solid and dashed curves, respectively, in Fig. 2 *A–C*. These calculations
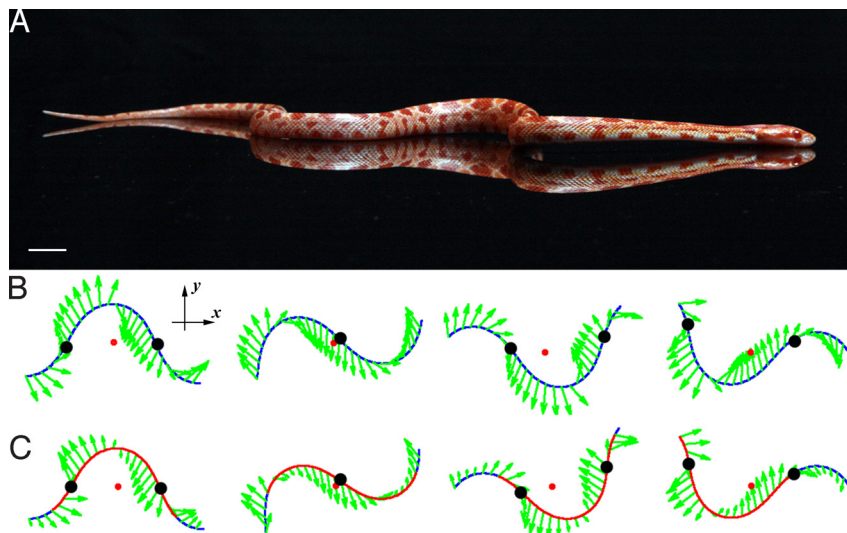
**Fig. 3.** Dynamic load distribution of the snake during lateral undulation. (*A*) A snake undulating on a mirrored surface, lifting the curves of its body. Although this technique was used to facilitate visualization rather than to study locomotion directly, a similar behavior is observed on rougher surfaces, on which the snake progresses easily. (Scale bar, 1 cm.) (*B* and *C*) Visualization of the calculated propulsive forces on a model snake with uniform (*B*) and nonuniform (*C*) weight distribution. Arrows indicate the direction and magnitude of the propulsive frictional force applied by the snake to the ground. Red lines indicate sections of the body with a normal force <1; the red dot indicates the center of mass. Inflection points of body shape, shown in black, show where the load is greatest. Note that in these simulations, although the weight distribution is nonuniform, the snake's body remains in contact with the ground everywhere along its body.

show that unloading of the model snakes' body leads to augmentation of forward speed $\bar{U}_{avg}$ from 0.17 to 0.23, an increase of 35% that is in greater accordance the observed speeds. Moreover, we find that the lifted snake has a mechanical efficiency $\eta$ of 0.29 compared with 0.20 for a nonlifted snake, an increase of nearly 50%, although this estimate does not account for the work required for the snake to lift its body. Fig. 3 *B* and *C* compares the frictional force distributions along the model snake in both the nonlifting and lifting gaits. It shows that lifting changes the direction of frictional forces of the parts of the snake that remain in firm contact with the ground. In particular, inflection points in shape (marked by black dots) where the load is greatest have an increased thrust component. Even with lifting, we do not fully account for the high range of snake speeds observed in the data ($\bar{U} = 0.15$–0.4, Fig. 2) although we did not attempt to optimize the weight distribution model. There are several other possible sources of modeling error or omission. For example, we have modeled the tail as having the same cross-section and mass per unit length as the body; if we include the actual tapering of the tail, the effective length $L$ of the snake decreases, worsening our speed prediction.

Another aspect that we have not considered is that snakes are likely able to dynamically change their frictional interactions with a surface by adjusting the attitude of their scales, a possibility that bears on our assumption of independent friction coefficients in Eq. **2**. As suggested by the theoretical predictions of motion on a ramp in Fig. 2*D*, which fit the experimental data better with forward friction coefficients of 0.3 rather than 0.1, snakes may be able to alter their frictional properties when moving up and down a slope.

## Statistical Methods

**Animals.** Ten juvenile Pueblan milk snakes (*Lampropeltis triangulum campbelli*, Fig. 1 *A* and *B*) of mass $15.2 \pm 2.6$ g (mean $\pm$ SE) and length $L$ of $36 \pm 2.3$ cm were obtained from a reptile breeder (Staten Island Serpents). Animals were housed singly in 2-L terrariums in an animal care facility and fed a diet of water and pinky mice. Animals were illuminated for 12 h per day and housed at $80 \pm 3.6$ °F, and humidity $23 \pm 10\%$.

**Friction Measurement.** Snakes underwent general anesthesia using 5% isoflurane provided by 1.0-Lpm $O_2$ in a 1-L chamber. Unconscious snakes were arranged in 9 orientations, from $\bar{\theta} = 0°$ to $\bar{\theta} = 180°$ on an inclined plane (Fig. 1*D*) covered with 2 materials, (*i*) a cloth whose characteristic length scale of roughness (0.2 mm) is comparable with the thickness of the snake's belly scales (0.1 mm) and (*ii*) a smooth fiberboard, whose scale of roughness 20 $\mu$m (27) is much less than that of the snake's scales. The edge of the inclined plane was lifted by hand until an inclination $\phi$ was reached at which the snakes began sliding; geometry shows that the static friction coefficient $\mu = \tan\phi$. Trials in which the snake rolled instead of slid were not analyzed; in all, 90 friction measurements were made.

**Slithering Observations.** Using a video camera (Sony), we observed snakes slithering over a plank $30 \times 120$ cm covered with either cloth or fiberboard, set at differing angles of inclination. Speeds of the center of mass were determined by image digitization and analysis using MATLAB. Movies in which the snake changed direction or gaits were not analyzed; in all, 70 films were of snake motion were analyzed.

1. Walton M, Jayne BC, Bennett AF (1990) The energetic cost of limbless locomotion. *Science* 249:524–527.
2. Cundall D (1987) Functional morphology in *Snakes: Ecology and Evolutionary Biology*, eds Siegel RA, Collins JT, Novak SS (Blackburn, Caldwell, NJ), pp 106–140.
3. Bellairs A (1970) *Life of Reptiles* (Universe Books, New York), Vol 2, pp 283–331.
4. Trueman ER (1975) *The Locomotion of Soft-Bodied Animals* (Edward Arnold, London).
5. Chan B, Balmforth NJ, Hosoi AE (2005) Building a better snail: Lubrication and adhesive locomotion. *Phys Fluids* 17:113101.
6. Gray J (1946) The mechanism of locomotion in snakes. *J Exp Biol* 23:101–120.
7. Gray J, Lissman HW (1950) The kinetics of locomotion of the grass-snake. *J Exp Biol* 26:354–367.
8. Jayne BC (1986) Kinematics of terrestrial snake locomotion. *Copeia*, 22:915–927.
9. Gans C (1984) Slide-pushing: A transitional locomotor method of elongate squamates. *Symp Zool Soc London* 52:12–26.
10. Mosauer W (1932) On the locomotion of snakes. *Science* 76:583–585.
11. Renous S, Hofling E, Gasc JP (1995) Analysis of the locomotion pattern of two microteiid lizards with reduced limbs, *Calyptommatus leiolepis* and *Nothobachia ablephara* (Gymnophthalmidae). *Zoology* 99:21–38.
12. Mahadevan L, Daniel S, Chaudhury MK (2004) Biomimetic ratcheting motion of a soft, slender, sessile gel. *Proc Natl Acad Sci USA* 101:23–26.
13. Guo ZV, Mahadevan L (2008) Limbless undulatory locomotion on land. *Proc Natl Acad Sci USA* 105:3179–3184.

14. Burdick JW, Radford J, Chirikjian GS (1993) A 'sidewinding' locomotion gait for hyper-redundant robots in *IEEE Int Conf Robot Autom* (IEEE, New York), pp 101–106.
15. Ostrowksi J, Burdick J (1996) Gait kinematics for a serpentine robot in *IEEE Int Conf Robot Autom* (IEEE, New York), pp 1294–1299.
16. Kuznetsov VM, Lugovtsov BA, Sher YN (1967) On the motive mechanism of snakes and fish. *Arch Ration Mech Anal* 25:367–387.
17. Rachevsky N (1938) *Mathematical Biophysics; Physico-Mathematical Foundations of Biology* (Dover, New York), Vol 2, pp 256–261.
18. Hirose S (1993) *Biologically Inspired Robots: Snake-Like Locomotors and Manipulators* (Oxford Univ Press, Oxford).
19. Hazel J, Stone M, Grace MS, Tsukruk VV (1999) Nanoscale design of snake skin for reptation locomotions via friction anisotropy. *J. Biomech (1999)*, 32:477–484.
20. Dowling KJ (1997) *Limbless Locomotion: Learning to Crawl with a Snake Robot.* PhD thesis (Carnegie Mellon Univ, Pittsburgh).
21. Choset HM (2005) *Principles of Robot Motion: Theory, Algorithms and Implementation* (MIT Press, Cambridge, MA).
22. Miller GSP (2002) Snake robots for search and rescue in *Neurotechnology for Biomimetic Robots*, eds Davis JL, Ayers J, Rudolph A (Bradford/MIT Press, Cambridge, MA), pp 269–284.
23. Alexander RM (2003) *Principles of Animal Locomotion* (Princeton Univ Press, Princeton).
24. Mosauer W (1935) How fast can snakes travel? *Copeia* 1935:6–9.
25. Childress S (1981) *Mechanics of Swimming and Flying* (Cambridge Univ Press, Cambridge, UK).
26. Secors SM, Jayne BC, Bennett AC (1992) Locomotor performance and energetic cost of sidewinding by the snake *Crotalus cerastes. J Exp Biol* 163:1–14.
27. Akbulut T, Ayrilmis N (2006) Effect of compression wood on surface roughness and surface absorption of medium density fiberboard. *Silva Fennica* 40(1): 161.